1 Title: Auditory Brainstem Mechanisms Likely Compensate for Self-imposed Peripheral
2 Inhibition
3
4 Abbreviated title: Brainstem Compensation of Peripheral Inhibition
5

6 **Authors** Abigayle Peterson[1,2], Vijayalakshmi Easwar[1,3], Lindsey Powell[1], and Sriram
7 Boothalingam[1,2]
8
9 *[1]Waisman Center and Department of Communication Sciences & Disorders*
10 *University of Wisconsin-Madison, Madison, WI 53705*
11 *[2]Macquarie University, Sydney, Australia*
12 *[3]National Acoustic Laboratories, Sydney, Australia*
13
14
15 **Corresponding Author:**
16 Sriram Boothalingam[1+]
17 sriram.boothalingam@mq.edu.au

18
19
20
21
22
23
24
25
26 **Conflict of interest statement**
27 The authors report no competing financial interests.
28
29
30

35
36
37
38
39
40
41
42
43
44
45

<u>Abstract</u>

46

47 It is well known that the medial olivocochlear reflex (MOCR) in the brainstem, part of the

48 efferent network, inhibits the cochlear active gain mechanism. The upstream neural influence of

49 this peripheral inhibition is less understood. When the MOCR is activated, responses generated

50 in the cochlea and cortex undergo putative attenuation, yet the amplitude of responses generated

51 in the brainstem are perplexingly unaffected despite decreased input from the periphery. Based

52 on known neural circuitry, we hypothesized that the inhibition of peripheral input is compensated

53 for by equivalent positive feedback in the brainstem over time. We predicted that the inhibition

54 can be captured at the brainstem with stimuli shorter (1.5 s) than previously employed long

55 durations (4 min) where this inhibition is diminished due to compensation. Results from 18

56 normal hearing human listeners support our hypothesis in that when the MOCR is activated,

57 there is a robust reduction of responses generated at the periphery, brainstem, and cortex for

58 short stimuli and that brainstem inhibition diminishes for longer stimuli. Our methodology and

59 findings have implications for auditory disorders such as tinnitus, evaluation of efferent function,

60 and provides a novel non-invasive window into potential gain compensation mechanisms in the

61 brainstem.

62

63

64

65

66

67

68

Introduction

69

70   Efferent neural networks fine-tune and regulate afferent sensory inputs. One such

71   network at the level of the brainstem, the medial olivocochlear reflex (MOCR), modulates

72   activity of one of the most peripheral auditory structures, the cochlear outer hair cells (OHCs).

73   The OHCs actively amplify basilar membrane motion for low-level sounds. When activated, the

74   MOCR inhibits this amplification process, thus turning down the cochlear gain. This reduction in

75   cochlear activity is thought to be useful for signal detection in noise (Winslow and Sachs, 1987;

76   Warren & Liberman, 1989) and protection against loud sounds (Rajan, 1988; Liberman, 1990;

77   Lauer and May, 2011). While the peripheral consequences of this inhibition are well-understood

78   from studies using measures such as otoacoustic emissions (OAEs) and auditory nerve

79   compound action potentials (CAPs), the upstream neural influence remains unknown, especially

80   in humans. As such, the goal of this study was to determine the central consequences of

81   peripheral MOCR inhibition. Our motivation stems from the need to uncover the ecological

82   relevance of MOCR inhibition. This requires an improved understanding of its effect along the

83   auditory pathway at different timescales.

84

85   It is well-established that stimulus-driven peripheral responses such as CAPs and OAEs

86   undergo robust attenuation when the MOCR is activated (Galambos, 1956; Warren & Liberman,

87   1989; Siegel and Kim, 1982; review: Guinan, 2006). However, current evidence perplexingly

88   exhibits a disparity of MOCR influence in the central systems based on the location of response

89   generation along the auditory neuraxis. For instance, endogenous components of cortical

90   responses (e.g., auditory steady state responses [ASSR] elicited at 40 Hz and thalamocortical

91   loop resonance in the gamma band), undergo considerable attenuation in the presence of putative

92   MOCR activation (Özdamar & Bohórquez, 2008; Ross et al., 2005, 2012; Maki et al., 2009).

93   However, sensory-driven neural responses that originate in the brainstem (e.g., ASSR elicited at

94   80 Hz and auditory brainstem response [ABR] wave V), appear unaffected under same testing

95   conditions (Özdamar & Bohórquez, 2008; Maki et al., 2009). This brainstem immunity to

96   MOCR effects, typically elicited by contralateral noise, remains unexplained. Here, we seek to

97   clarify our hypothesis that brainstem-dominant neural responses show immunity because local

98   feedback networks in the brainstem compensate for the peripheral inhibition.

99

100   The rationale for our hypothesis is rooted in (1) previously identified circuits that are

101   capable of such compensation (Fujino & Oertel, 2001; Hockley et al., 2021), and (2) gain

102   compensation that occurs for more extreme peripheral input loss due to pathologies such as

103   cochlear ablation, deafferentation, and conductive loss (Chambers et al., 2016; Parry et al., 2019;

104   Sheppard et al., 2019). We predict that if local feedback networks do compensate for the MOCR-

105   mediated peripheral inhibition, a latency between stimulus presentation, peripheral inhibition,

106   and complete compensation would be apparent. Based on the time (~400 ms) it takes for the

107   MOCR inhibition on OHCs to stabilize (Boothalingam et al., 2021; Backus and Guinan, 2006),

108   we speculated that the time taken for complete compensation will fall between 0.5 and a few

109   seconds. To test this prediction, we concurrently measured peripheral (cochlear) and neural

110   (brainstem or cortical) responses in short (1.5 s) and long (4 mins) click-trains. Our results

111   support our hypothesis in that, responses at the periphery (OAEs at 40 and 80 Hz), brainstem (80

112   Hz ASSRs) and the cortex (40 Hz ASSRs) demonstrate robust inhibition in shorter durations,

113   however, for longer durations, only the inhibition of brainstem responses diminishes. That is, the

114   inhibition appears to be compensated for at the brainstem between 1.5 s and 4 mins. This

115   approach likely provides a window into brainstem feedback circuits that are involved in

116   enhancing the peaks of complex signals (e.g., speech) and possibly maintaining the homeostasis

117   in response to a, self-imposed, decrease in auditory input from the periphery (Brown, 2011;

118   Fujino & Oertel, 2001; Hockley et al., 2021). In addition, our non-invasive, approach offers a

119   solution to evaluating auditory efferent function in patients with sensorineural hearing loss and

120   offers a new perspective on the ecological relevance of the MOCR.

121

122   **Materials and Methods**

123   **Participants**

124   Twenty young, clinically normal-hearing adults participated in the study. Clinically

125   normal hearing was established by an unremarkable otoscopic examination, bilateral hearing

126   thresholds ≤20 dB HL at octave frequencies from 0.25 to 8 kHz (SmartAuD, Intelligent Hearing

127   Systems [IHS], FL, USA), normal middle ear function as measured by tympanometry (Titan,

128   Interacoustics, Denmark), measurable (magnitude greater than 0 dB with at least 6 dB signal-to-

129   noise ratio [SNR]) distortion product OAEs (0.5-6 kHz at 65/55 dB SPL, SmartDPOAE, IHS,

130   FL), and self-report of no neurological disorders. Two participants were rejected from analysis

131   due to excessive noise in OAEs, reducing the number of participants to 18 (mean age ± standard

132   deviation [SD]) = 22.3±3 years; 1 male). Participants were either offered extra credit for their

133   participation or compensated at the rate of $10/hour. The study procedures were approved by the

134   University of Wisconsin-Madison Health Sciences Institutional Review Board. Written consent

135   was obtained from all participants prior to data collection.

136

137   **Stimuli**

138   All stimuli were digitally generated in MATLAB (v2017b; Mathworks, MA, USA) at a

139   sampling rate of 96 kHz and a bit-depth of 24. The stimuli used to elicit OAEs and ASSRs were

140   click trains with click rates of either 40 or 80 Hz presented at 65 dB peak-to-peak (pp) SPL.

141   Whereas the 40 Hz clicks elicit a predominantly cortical response, the 80 Hz clicks elicit a

142   predominantly brainstem response (Bidelman, 2018; Herdman et al., 2002; Kuwada et al., 2002;

143   review: Dimitrijevic and Ross, 2008). Although henceforth we will refer to 40 Hz vs. 80 Hz

144   responses as synonymous with cortical vs. brainstem sources for brevity given previously

145   established dominant neural sources, it is acknowledged that both scalp-recorded responses

146   reflect multiple neural generators. The clicks were bandlimited between 0.8 and 5 kHz to focus

147   the stimulus energy on frequency regions where the MOCR function is most prominent, when

148   measured using OAEs (Lilaonitkul and Guinan, 2012; Zhao and Dhar, 2012). Bandlimited clicks

149   were generated in the frequency domain using a recursive exponential filter (Zweig and Shera,

150   1995; Charaziak et al., 2020) and inverse Fourier-transformed to the time domain. The duration

151   of the click was ∼108 μs. Clicks were presented in positive and negative polarities to reduce

152   potential contamination with stimulus artifact when averaging for ASSRs. Broadband noise

153   (0.001 to 10 kHz) was presented at 60 dB SPL in the contralateral ear to elicit the MOCR. Both

154   the ipsilateral clicks and the contralateral noise are illustrated in Fig. 1. In-ear calibration was

155   performed for clicks to ensure the peak-to-peak level of the click stimulus was 65 dB ppSPL in

156   all participants. Broadband noise was calibrated in an ear simulator (Type 4157, Bruel & Kjaer,

157   Denmark).

158

159   **Instrumentation**

160   Stimuli were generated, delivered and controlled through an iMac computer (Apple, CA,

161   USA) running Auditory Research Lab Audio Software (ARLas v4.2017; Goodman, 2017) on

162   MATLAB. The iMac was interfaced with an external sound card (Fireface UFX+; RME,

163   Germany) via thunderbolt for analog-to-digital-to-analog conversion at a sampling rate of 96

164   kHz. Clicks were presented in the ipsilateral ear via one of the miniature loudspeakers of the

165   ER10C+ (Etymotic Research, IL, USA) system. Ear canal pressures were registered and

166   amplified (+20 dB) by the ER10C+ probe microphone placed in each ear. To avoid changes in

167   stimulus level over the course of the experiment, the probe placement was secured in the ear

168   using foam tips and using silicone putty around the probe in-ear (Silicast, Westone Laboratories,

169   CO; Boothalingam and Goodman, 2021). The MOCR eliciting broadband noise was presented in

170   the contralateral ear using an ER2 (Etymotic Research, IL) insert earphone coupled with a foam

171   tip of appropriate size.

172

173   Electroencephalography (EEG) amplitude was registered by the Universal Smart Box

174   (USB; IHS, FL, USA) controlled by a PC equipped with the Continuous Acquisition Module

175   (IHS, FL, USA) at the sampling rate of 10016 Hz. One of the IHS USB channels recorded

176   triggers (5V impulses) that coincided with the onset of stimulus blocks to index EEG data

177   accurately. A single-channel montage was used for EEG acquisition with three sintered Ag-AgCl

178   electrodes. The vertex (Cz) was used as the non-inverting electrode site and the nape was used as

179   the inverting site (Picton et al., 2003). The left collarbone was used as the ground. All electrode

180   sites were cleaned with alcohol wipes and scrubbed with a mild abrasive gel (Nuprep) prior to

181   affixing electrodes with adhesive sleeves and conduction gel (SignaGel). Electrode impedances

182   were monitored throughout the experiment and were always <3 kΩ at each site.

183

Experimental Design

184

185   The experiment was conducted in a double-walled sound-attenuating booth where

186   participants sat comfortably in a recliner for the duration of the experiment. Participants were

187   instructed to sit relaxed, not move, swallow as few times as comfortable during stimulation, and

188   maintain a wakeful state (watching a silent, closed caption movie). As shown in Fig. 1, OAEs

189   and ASSRs were measured at 40 and 80 Hz with and without contralateral noise, in short (1.5 s)

190   and long (4 min) durations. The conditions (rate and duration) alternated between clicks with and

191   without contralateral noise separated by 0.5 s of silence, and was repeated in positive and

192   negative polarities. The long condition was a single block of 4 min recording completed

193   separately for with- and without-contralateral noise, i.e., no repetitions. In contrast, in the short

194   condition, 1.5 s-long click trains were repeated 160 times to match the total number of clicks

195   presented in the respective long condition. This was done to avoid SNR differences in responses

196   between long and short conditions analyzed in the frequency domain. The order of presentation

197   in short/long conditions was counter-balanced but the 40 Hz short duration was always

198   completed first to ensure maximum wakeful participant state as 40 Hz can be attenuated by sleep

199   (Picton et al., 2003). The stimulus ear was chosen based on the ear with the largest DPOAE

200   amplitude obtained during screening. The experimental procedure took about two hours with

201   breaks, as desired by the participant, between conditions.

202

Response Analysis

203

204   OAEs were extracted from click 'epochs', defined as the duration between two

205   successive clicks. OAE analysis was performed offline in MATLAB using custom scripts. Raw

206   ear canal pressure recording was bandpass filtered around the click frequency (0.8–5 kHz). An

207   artifact rejection, where clicks with a root-mean-square (RMS) amplitude that fell outside the

208   third quantile + 2.25 times the interquartile range (specific to the condition and within

209   participants) were excluded from further analysis. Typically, less than 10% of the responses were

210   rejected across participants. Data was grouped by duration with or without contralateral noise.

211   The stimulus (0–4ms) and OAEs (6.5–12.5ms) were then separated for further analysis for both

212   40 and 80 Hz rates. Specifically, OAEs were used to determine the presence of the MOCR. The

213   click stimulus was used to determine the presence of the middle ear muscle reflex (MEMR) that

214   can potentially confound MOCR effects on OAEs (Boothalingam et al., 2018).

215

216   OAE amplitude was estimated as the RMS of ear canal pressure between 6.5–12.5 ms

217   and the noise floor was estimated by the mean difference of two OAE RMS buffers (even and

218   odd-numbered epochs). Prior to estimating the RMS amplitude, OAEs were considered in the

219   frequency domain to extract OAEs 12 dB above the noise floor to ensure the MOCR-mediated

220   inhibition was estimated only from high quality OAEs (Guinan, 2012; Goodman et al., 2012;

221   Boothalingam et al., 2021). For each duration and rate condition, the RMS of OAE and stimulus

222   amplitude (dB SPL) with noise were subtracted from the RMS without noise to compute the

223   effect of MOCR and MEMR (in dB), respectively.

224

225   The same pre-processing strategy as ear canal pressure was applied to the raw EEG data.

226   Raw EEGs were chunked into 1.5-s or 4-min epochs corresponding to short and long durations,

227   respectively. Chunked EEGs were averaged over opposite stimulus polarities to minimize any

228   stimulus artifacts. Finally, ASSR amplitudes were determined from the Fourier transforms of the

229   averaged EEGs across with and without noise estimates at 40 and 80 Hz. EEG noise floor was

230   estimated as the average of 8 frequency bins around the ASSR frequencies (Picton et al., 2003).

231   The reduction in response amplitude with contralateral noise relative to no-noise condition is

232   henceforth referred to as 'inhibition' in both OAEs and ASSRs.

233

Middle ear muscle reflex (MEMR) estimation

235   When elicited by high level sound, the MEMR stiffens the ossicular chain, altering signal

236   transfer through the middle ear (Boothalingam et al., 2021; Borg, 1968) and may thus confound

237   MOCR effects on OAEs (Boothalingam et al., 2021; Goodman et al., 2013; Guinan et al., 2003).

238   The click stimulus (0–4 ms) in the same frequency range as the OAEs was analyzed to determine

239   the presence of MEMR. The same analyses as OAEs were applied to obtain stimulus level across

240   conditions. To evaluate if the MEMR influenced OAEs, we performed two tests. First, a 3-way

241   repeated measures analysis of variance (RM-ANOVA) was performed to test if the MEMR

242   magnitude varied as a function of independent variables duration, click rate, and contralateral

243   noise. Our results show that none of the main effects and interactions were significant (p>0.05).

244   This suggests that the variables in the study did not systematically influence the stimulus level,

245   therefore, even if any MEMR was activated, it did not influence our results. Second, Pearson

246   correlations were performed to evaluate the relation between any change in stimulus amplitude

247   on OAEs. As seen in Fig. 2, none of the correlations, except the long condition at 80 Hz, were

248   significant suggesting that the changes in stimulus level did not influence changes in OAE level.

249   For the significant correlation at long/80 Hz, removing the one outlier made the correlation non-

250   significant (Fig. 2., panel C). Clearly, for this one participant, MEMR likely influenced the OAE

251   change in this one condition. However, we did not exclude this data for further analysis below

252   because (1) this is not consistent across conditions, (2) the influence is on the direction opposite

253   to what is expected – increase in OAE level as opposed to a reduction, and (3) because group

254   effects were not significant (3-way ANOVA). Taken together, the OAE changes presented in this

255   study are driven by the MOCR and not the MEMR.

256   **__Results__**

257   ASSR and OAE amplitudes are plotted as a function of click rate (40 vs. 80 Hz),

258   contralateral noise (with vs. without), and duration (long vs. short) in Fig. 3. Notice the marked

259   reduction in both OAE and ASSR amplitudes in the long condition. This reduction appears

260   relatively unchanged for OAEs between short and long conditions. A 3-way repeated measures

261   analysis of variance (ANOVA) for ASSRs revealed a significant three-way interaction. That is,

262   the effect of noise varied as a function of duration and rate ($F[1, 17])=33.28, p<0.001$). Post-hoc

263   t-tests were corrected for multiple comparisons using the False Discovery Rate (FDR; Benjamini

264   and Hochberg, 1995). We report FDR corrected p-values and hence $p<0.05$ are to be interpreted

265   as significant. These post-hoc tests demonstrate a significant effect of noise on 40 Hz ASSR in

266   both short ($p<0.001$) and long ($p=0.03$) durations, however, the effect of noise on 80 Hz ASSR

267   was only significant for the short ($p<0.001$) but not long ($p=0.486$) duration.

268   A 3-way repeated measures ANOVA on OAE amplitude showed no significant 3-way

269   interaction but the two-way interaction between duration and click rate ($F[1, 17]= 13.2,$

270    $p=0.002$) and the two-way interaction between duration and noise ($F[1, 17]=8.81, p=0.008$)

271   were significant. Further, OAE amplitude also varied as a main effect of noise ($F[1, 17] = 58.5,$

272    $p<0.001$) suggesting and peripheral inhibition through MOCR activation, as expected. Post-hoc

273   *t*-tests suggest the effect of noise on OAE amplitude was significant for both short ($p<0.001$) and

274   long ($p<0.001$) durations when averaged over both rates.

275   To investigate the influence of MOCR inhibition at the periphery (OAEs) on the

276   inhibition at brainstem (80 Hz ASSR) and cortical (40 Hz ASSR) levels, we performed

277   correlations. These relations are plotted in Fig. 4. ASSR and OAE inhibition were not correlated

278   for the 40 Hz short condition ($p=0.454$), the 40 Hz long condition ($p=0.962$), and the 80 Hz long

279   condition ($p=0.981$). However, the change in OAEs and ASSRs was positively correlated in the

280   80 Hz short duration condition ($p=0.045$). Although the *p*-value is only marginally significant for

281   this correlation, the coefficient ($r=0.48$) is consistent with a moderate-to-large effect (Cohen,

282   1988) and the trend in the data (Fig. 4) is quite apparent unlike the other non-significant

283   correlations. This result likely suggests that changes observed in ASSRs generated

284   predominantly at the cortex (40 Hz) are likely not influenced by MOCR-induced OAE changes

285   at the periphery. However, for ASSRs generated predominantly at the brainstem (80 Hz), the

286   changes at the periphery likely influence neural activity when viewed in shorter time intervals,

287   but this washes out when observed over a longer time window.

288   The relation between the short and long durations for ASSRs and OAEs in the magnitude

289   of inhibition are shown in Fig. 5. There was a significant positive correlation between OAE

290   inhibition in short and long durations observed for both 40 Hz ($p<0.001$) and 80 Hz ($p=0.001$)

291   rates. This indicates that individuals exhibited similar OAE inhibition magnitudes in long and

292   short durations, likely due to a single mechanism, the MOCR, influencing activity at the

293   periphery. However, this relationship was not observed for the ASSR inhibition between short

294   and long for 40 Hz ($p=0.770$) or 80 Hz ($p=0.346$), suggesting differential effects of the eliciting

295   contralateral noise depending on the duration of stimulus presentation.

296   We also compared inhibition between the two click rates within short and long durations

297   and separately for ASSRs and OAEs to investigate if any relationships exist between rates. That

298   is to test if responses generated at various levels of the auditory pathway are related in the

299   manner they are measured in this study. The comparisons and correlations are plotted in Fig. 6.

300   For ASSRs, there was no correlation between the inhibition at both click rates for ASSR short

301   ($p=0.299$) and long ($p=0.434$) durations, as expected. This likely indicates that amplitude

302   changes observed in cortical-dominated (40 Hz) ASSRs are independent of brainstem-dominated

303   (80 Hz) ASSR changes in both time durations. For OAEs, while there was a significant

304   correlation between 40 and 80 Hz in the short condition ($p=0.020$), the correlation in the long

305   condition was not significant ($p=0.961$), consistent with the interaction between rate and

306   duration in the ANOVA for OAEs. Taken together, these results align with our hypothesis that

307   brainstem mechanisms likely compensate for self-imposed peripheral inhibition.

308

Discussion

310   By monitoring cochlear, brainstem and cortical activity with and without MOCR

311   activation in short and long stimulus durations (1.5 s and 4 mins), we found (1) significant

312   inhibition at the periphery and cortex, but not at the brainstem, with long duration stimuli,

313   consistent with previous studies (Özdamar & Bohórquez, 2008; Kawase et al., 2012; Maki et al.,

314   2009; Ross et al., 2005, 2012; Usubuchi et al., 2014), and (2) significant inhibition at the

315   periphery, cortex and notably the brainstem, with short duration stimuli. Below, we discuss these

316   results based on known gain compensation circuits at the brainstem reported in animal models

317   (Hockley et al., 2021; Fujino and Oertel, 2001) and potential alternative reasons.

318

319   **Gain compensation in the brainstem**

320   In contrast to the 40 Hz ASSR, the 80 Hz ASSR demonstrates differential inhibition

321   based on the stimulus duration. Methodologically, the total duration of stimulus presentation was

322   equalized between the long and short duration conditions and therefore does not warrant the

323   observed differential effect. In addition, at the periphery, the MOCR inhibition of OAEs across

324   rates and durations is indistinguishable. Given the lack of methodological differences and

325   similarity in peripheral MOCR inhibition between the two durations, the differential effect of

326   noise on the 80 Hz, but not 40 Hz ASSR, can be conjectured to arise either (1) from the

327   difference in the sensitivity of the respective generators to contralateral noise or (2) second-

328   degree factors that influence the generated ASSR differentially between brainstem and more

329   rostral centers.

330

331   Previous studies have demonstrated generator-specific effects of contralateral noise.

332   Notably, Özdamar & Bohórquez (2008) showed robust attenuation of later occurring components

333   (Pb) of the middle latency responses elicited at 40 Hz, presumably generated in the cortex.

334   However, such an effect was not observed for concurrently measured ABR wave-V, generated in

335   the brainstem. Similarly, Galambos and Makeig (1992) reported significant attenuation of click-

336   evoked 40 Hz ASSR but not concurrently recorded ABRs. Maki et al. (2009), like the present

337   study compared attenuation of 40 and 80 Hz ASSRs to contralateral noise. They reported

338   reduction of 40 Hz ASSRs but no effect of the contralateral noise on 80 Hz ASSRs. Speculations

339   for such disparity in noise effects on responses generated at the brainstem vs. the cortex has been

340   attributed to one of two reasons. It is possible that noise effects must occur more rostral to the

341   ABR generation site (brainstem; Galambos and Makeig, 1992; Usubuchi et al., 2014), i.e., the

342   generators themselves must be different or that any peripheral inhibition by the MOCR is

343   insignificant for neural measures (Özdamar & Bohórquez, 2008).

344

345   The speculation that noise-mediated inhibition of neural responses, also referred to as

346   central masking, occurring only rostral to the brainstem (Galambos and Makeig, 1992; Usubuchi

347   et al., 2014) does not explain the differential noise effects for different types of cortical

348   responses. For instance, although Usubuchi et al. (2014) found significant inhibition for both 20

349   and 40 Hz neuromagnetic ASSRs, the effect of contralateral noise was more pronounced for the

350   40 Hz response. While comparing the neuromagnetic 40 Hz ASSRs and the sensory-driven N100

351   response, Kawase et al. (2012) found robust inhibition of 40 Hz with contralateral noise but no

352   effect on the N100. However, Okamoto et al. (2005) was demonstrated inhibition of the same

353   neuromagnetic N100 like many EEG estimates of N100 (e.g., Salo et al., 2003; Rao et al., 2020).

354   A notable difference between Okamoto et al. (2005) and Kawase et al. (2012) is that Okamoto et

355   al. (2005), apart from studying notch width effects of the noise, use a paradigm that is more akin

356   to our short interval condition where the effect of noise was captured on the test stimulus within

357   0.5s. In general, there appears to be variable effects of contralateral noise even within responses

358   generated in the cortex and thalamocortical regions. This suggests that other second-degree

359   factors, likely both stimuli-based (e.g., stimulus duration) and physiology-based (e.g., phase reset

360   hypothesis on 40 Hz generation; Ross et al., 2005), are at play in the contralateral noise-mediated

361   inhibitory effects on cortical activity. These factors might also apply for the differences in noise

362   effects observed between cortex- vs. brainstem-generated ASSRs in the present study simply by

363   virtue of the two generators being different. The different generator, however, does not support

364   contralateral noise sensitivity to structures only rostral to the brainstem.

365

366   The argument for OHC inhibition by the MOCR being insignificant for neural inhibition

367   (Özdamar & Bohórquez, 2008) also does not explain the disparity in noise effects across neural

368   response generators because (1) the present study results show significant attenuation of 80 Hz

369   ASSRs when acquired in short time intervals and (2) attenuation of auditory nerve compound

370   action potentials is an established marker of MOCR activity on the afferent auditory pathway

371   (Galambos, 1956; Guinan and Gifford, 1988; Liberman, 1989). As such, MOCR-mediated

372   inhibition of OHC amplifier gain is indeed reflected in the auditory nerve response. Therefore, it

373   is still perplexing that the MOCR-mediated attenuation is absent for responses generated at the

374   brainstem when averaged over minutes, especially when it is present (1) at areas rostral to the

375   brainstem, and (2) when responses at the brainstem are considered in shorter time intervals.

376

377   Our results may, for the first time, provide a reasoning for the perplexing "insignificant"

378   effect of the MOCR on brainstem generated evoked potentials. Consistent with our hypothesis,

379   we posit that the MOCR-mediated peripheral inhibition probably does become insignificant at

380   the brainstem because mechanisms in the brainstem compensate for the loss in input at the

381   periphery. Known feedback circuitry in the cochlear nucleus support our hypothesis. Based on

382   positive feedback loops between the cochlear nucleus and the superior olivary complex identified

383   in previous animal studies, the likely candidates for such compensation would be the T-stellate

384   (Fujino & Oertel, 2001; Brown, 2011) and the small cells (Hockley et al., 2021).

385

386   Anatomically, both T-stellate and small cells of the CN receive direct inputs from the

387 auditory nerve (Liberman, 1991; Blackburn and Sachs, 1989), project to MOC neurons (Romero

388 and Trussell, 2021; de Venecia, et al., 2005; Benson and Brown, 2006; Thompson and

389 Thompson, 1991; Darrow et al., 2011), and receive collaterals from MOC neurons (Benson and

390 Brown, 1990; 1992; Benson et al., 1995; Fujino and Oertel, 2001). These projections and inputs

391 create positive feedback loops for both cell types (i.e., T-stellate-MOC-T-stellate and small cell-

392 MOC-small cell). However, Hockley et al. (2021) reported that activating MOC neurons

393 increased excitation of small cells, but not T-stellate cells. This is intriguing given prior evidence

394 for profuse amounts of MOC collaterals to multipolar/chopper/T-stellate cells (Fujino & Oertel,

395 2001; Benson and Brown, 1990; review: Brown, 2011). Hockley et al. (2021) do not report how

396 activities of the two CN cell types vary across time scales (e.g., seconds to minutes). Regardless,

397 it is clear that MOC neurons retroactively excite CN neurons, quite likely the same neurons that

398 excite them. In addition, both the MOC neurons and T-stellate cells project to the inferior

399 colliculus (IC) (Schofield, 2001; Okoyama et al., 2006), and a recent study suggests that inputs

400 from CN and IC together optimize MOC activity (Romero and Trussell, 2021). The projection to

401 the IC is important because it is a major generation site for 80 Hz ASSRs (Bidelman, 2018;

402 Herdman et al., 2002; Kuwada et al., 2002; review: Dimitrijevic and Ross, 2008) and is in the

403 vicinity of the ABR wave-V generator (Moller and Jannetta, 1982).

404

405 **Relevance of gain compensation at the brainstem**

406   The putative positive MOCR feedback loops for both cell types, the T-stellate and small

407 cells, are thought to act as 'efferent copies' of MOCR inhibition at the periphery and likely

408 compensate for the reduced input (Brown, 2011; Fujino and Oertel, 2001). This gain

409 compensation could be critical for at least three reasons. First, a reduction of input at the

410 periphery will decrease excitation of the MOCR and the MEMR, which will in turn limit their

411 functional ability to protect vulnerable cochlear hair cells from acoustic overexposure (Rajan,

412 1988; Liberman, 1990; Lauer and May, 2011; Brown, 2011; Fujino and Oertel, 2001). Second, a

413 reduction of input at the periphery might negatively impact central gain, and possibly the tuning

414 of the T-stellate cells (Rhode and Greenberg, 1994) as it would alter the input to D-stellate cells.

415 By providing inhibitory input to the T-stellate cells, the D-stellates provide a balance in gain in

416 the CN among their various other functions (Ferragamo et al., 1998; Oertel et al., 2011; Rhode

417 and Greenberg, 1994). Reduced T-stellate cell inhibition, combined with the recently discovered

418 excitatory loop gain within T-stellate cells (Cao et al., 2019) could lead to tinnitus and

419 hyperacusis when left unchecked (Hockley et al., 2021). Third, compensating for reduced

420 peripheral input likely restores, and possibly enhances, the fidelity of the sound level,

421 specifically the spectral peaks as encoded by T-stellate cells (Blackburn and Sachs, 1990; May et

422 al., 1998; Oertel et al., 2011) and small cells (Hockley et al., 2021). At a population level, both

423 T-stellate cells and small cells encode spectral peaks and have been identified to be critical for

424 speech perception (Hockley et al., 2021; Oertel et al., 2011; May, LePrell, and Sachs, 1998;

425 Blackburn and Sachs, 1990). The MOC neurons only provide cholinergic input to the T-stellate,

426 not D-stellate cell, which is thought to lead to selective enhancement of spectral peaks and not

427 valleys, improving the overall SNR in the system (Fujino and Oertel, 2001). Further, T-stellate

428 and small cells respond optimally at moderate to high stimulus levels, like the elicitor used in the

429 present study (60 dB SPL; Lai, Winslow, and Sachs, 1994; Liberman, 1991; Ryugo, 2008) and

430 are, therefore, likely to be reflected in our experimental approach.

431

432 Taken together, the compensation mechanisms likely reflected in our results are critical

433 for maintaining homeostasis, continued protection of peripheral structures, and prevent

434 peripheral inhibition from degrading the encoding of important acoustic information. By

435 contrasting short vs. long duration conditions, our results provide a potential non-invasive

436 window into these mechanisms. As with any non-invasive markers, their true physiological

437 origins must be established using direct and likely invasive studies of these systems. Specifically,

438 future studies capable for selectively silencing the feedback from the T-stellate and small cells in

439 the CN to the MOCR may provide the most conclusive evidence for our hypothesized gain

440 compensation mechanism.

441

442 **If the brainstem compensates, why is inhibition still present at the brainstem and the**

443 **cortex?**

444 If the inhibition of peripheral input is compensated for in the CN, the inhibition of

445 brainstem-generated (80 Hz) ASSRs observed in the short duration condition reveals a time

446 course to this compensation. Currently, there are no studies that directly describe the

447 physiological time course of T-stellate/small cell-MOCR-mediated gain compensation.

448 Nevertheless, the pattern of results in this study may be explained by the established kinetics of

449 the MOCR pathway. It can be conjectured that inhibition of auditory nerve inputs by the MOCR

450 causes an initial reduction in inputs to the CN, likely on a scale of several tens to a few hundred

451 milliseconds, commensurate with the MOCR activation time course of 200-250 ms and the

452 roughly 400 ms it to reach steady state (Backus and Guinan, 2006; Boothalingam et al., 2021).

453 Considering that both the MOCR and T-stellate cells integrate energy over time and continue to

454   be excited even after stimulus cessation, the gain compensation could happen over a few

455   seconds. This initial reduction in peripheral input is reflected as reduced brainstem-dominated

456   ASSR amplitude (80 Hz) in the short duration condition and is somewhat supported by the

457   positive correlation with MOCR inhibition of OAEs in this condition (Fig 4D).

458

459   When contralateral noise was introduced, a reduction in cortex-generated (40 Hz) ASSR

460   amplitude was observed with both long stimulus durations consistent with previous studies

461   (Galambos & Makeig, 1992; Ross & Fujioka, 2016; Maki et al., 2014; Usubuchi et al., 2009), as

462   well as with short stimulus durations. However, the lack of significant correlation between the

463   change in ASSR amplitude for 40 Hz and OAEs (Fig 4) suggest that the reduction in 40 Hz

464   ASSR amplitude is unlikely to be related to the MOCR-mediated peripheral inhibition. This

465   finding corroborates the findings of Mertes and Leek (2016) and Mertes and Potocki (2022) –

466   significant reduction in 40 Hz ASSR without any correlation with the inhibition of OAEs. The

467   reduction of 40 Hz ASSR amplitude may instead be explained by an interruption in

468   thalamocortical loop resonance induced by contralateral noise. Desynchronization of 40 Hz

469   ASSR, associated with a temporary decrease in the amplitude of oscillatory signal power in

470   response to a concurrent stimulus, was similarly observed by Ross and colleagues (2005; 2012).

471   ASSR desynchronization is a general reaction to both new and changing stimuli (Ross et al.,

472   2005) thought to act as a reset to the adaptation of auditory processing (Rogers & Bregman,

473   1998). The reduction in 40 Hz ASSR amplitude may reflect this temporary desynchronization,

474   which is more evident when averaging amplitude over short compared to long durations.

475

Clinical implications of a non-invasive window into brainstem gain compensation

Considering the role that peripheral input to the CN plays in the gain compensation mechanism, the impact of hearing loss should be further investigated for diagnostic/therapeutic implications and for uncovering the mechanism's ecological purpose. For instance, in the case of sensorineural hearing loss resulting from outer hair cell damage, MOCR inhibition would not affect the outer hair cell activity, but the gain compensation may still enhance T-stellate and small cell excitation. This process may result in a net positive excitation – overcompensation – in the CN. This overcompensation may contribute to auditory disorders characterized by hyperactivity such as tinnitus and hyperacusis (Noreña, 2011; Zeng, 2013; Cao et al., 2019; Hockley et al., 2021).

MOCR function is important to consider in a clinical setting as it has been hypothesized to improve speech perception in noise (Giraud et. al., 1997: Kumar and Vanaja, 2004; Mishra and Lutman, 2014). Prior arguments for an MOCR role in speech perception were based only on its ability to restore the dynamic range of the auditory nerve (Guinan, 2006). Evidence of MOCR collateral activity in CN – enhancing T-stellate and small cell output – further strengthens the role of MOCR in speech perception (Fujino and Oertel, 2001; Hockley et al., 2021). OAEs are typically used to measure the MOCR strength in normal hearing individuals. Given that OAEs rely on OHC activity, hearing loss due to OHC damage emphasizes the need for alternative measures of MOCR function. While ASSRs appear to be a promising alternative, our findings indicate that the time scale and generation site at which inhibitory effects are compensated for must be carefully considered. For instance, the contralateral noise-mediated inhibition of 40 Hz ASSRs (Mertes and Leek, 2016; Mertes and Potocki, 2022; Usubuchi et al., 2014; Maki et al.,

498   2009) may not reflect MOCR inhibition of OHC activity (Fig 4) as any reduction in peripheral

499   input to the cortex is likely iteratively compensated for at the brainstem.

500

501   In summary, our findings offer a potential new window into a gain compensation

502   mechanism in the brainstem previously identified in animal models. Additionally, this study

503   demonstrates the ability of the 80 Hz ASSR to measure MOCR function using short duration

504   stimuli. Our methods and corresponding results also emphasize the importance of timescale

505   consideration for future research utilizing ASSRs to measure the MOCR.

506   **References**

507   Backus, B. C., & Guinan Jr, J. J. (2006). Time-course of the human medial olivocochlear reflex.

508   *The Journal of the Acoustical Society of America*, 119(5), 2889-2904.

509   Benson, T. E., & Brown, M. C. (1990). Synapses formed by olivocochlear axon branches in the

510   mouse cochlear nucleus. *Journal of Comparative Neurology*, 295(1), 52-70.

511   Benson, T. E., & Brown, M. C. (2006). Ultrastructure of synaptic input to medial olivocochlear

512   neurons. *Journal of Comparative Neurology*, 499(2), 244-257.

513   Bidelman, G. M., Jennings, S. G., Lopez-Poveda, E. A., Smith, S. B., Lichtenhan, J. T., & Cone,

514   B. K. (2017). Contralateral Inhibition of Click- and Chirp-Evoked Human Compound

515   Action Potentials. *Frontiers in Neuroscience*, *11*, 189.

516   https://doi.org/10.3389/fnins.2017.00189

517   Bidelman, G. M. (2018). Subcortical sources dominate the neuroelectric auditory frequency-

518   following response to speech. *Neuroimage*, *175*, 56-69.

519   Blackburn, C. C., & Sachs, M. B. (1990). The representations of the steady-state vowel

520   sound/e/in the discharge patterns of cat anteroventral cochlear nucleus neurons. *Journal of*

521   *neurophysiology*, 63(5), 1191-1212.

522   Özdamar, O. & Bohórquez, J. (2008) Suppression of the Pb (P1) component of the auditory

523   middle latency response with contralateral masking. *Clinical Neurophysiology* **119**, 1870–

524   1880.

525   Boothalingam, S., Kurke, J., & Dhar, S. (2018). Click-evoked auditory efferent activity: Rate and

526   level effects. Journal of the Association for Research in Otolaryngology, 19(4), 421-434.

527

528   Boothalingam, S., Goodman, S. S., MacCrae, H., & Dhar, S. (2021). A Time-Course-Based

529   Estimation of the Human Medial Olivocochlear Reflex Function Using Clicks. *Frontiers in*

530   *Neuroscience*, 15.

531   Borg, E. (1968). A quantitative study of the effect of the acoustic stapedius reflex on sound

532   transmission through the middle ear of man. Acta oto-laryngologica, 66(1-6), 461-472.

533   Brown, M. C. (2011). Anatomy of olivocochlear neurons. In *Auditory and vestibular efferents*

534   *(pp. 17-37)*. Eds. D. K. Ryugo, R. R. Fay, and A. N. Popper. Springer, New York, NY.

535   Cao, X. J., Lin, L., Sugden, A. U., Connors, B. W., & Oertel, D. (2019). Nitric oxide-mediated

536   plasticity of interconnections between t-stellate cells of the ventral cochlear nucleus

537   generate positive feedback and constitute a central gain control in the auditory system.

538   *Journal of Neuroscience*, 39(31), 6095-6107.

539   Chambers, A. R., Resnik, J., Yuan, Y., Whitton, J. P., Edge, A. S., Liberman, M. C., & Polley,

540   D. B. (2016). Central Gain Restores Auditory Processing following Near-Complete

541   Cochlear Denervation. *Neuron*, *89*(4), 867–879.

542   https://doi.org/10.1016/J.NEURON.2015.12.041

543   de Boer, J., Thornton, A. R. D., & Krumbholz, K. (2012). What is the role of the medial

544   olivocochlear system in speech-in-noise processing? *Journal of Neurophysiology*, *107*(5),

545   1301–1312. https://doi.org/10.1152/JN.00222.2011

546   De Venecia, R. K., Liberman, M. C., Guinan Jr, J. J., & Brown, M. C. (2005). Medial

547   olivocochlear reflex interneurons are located in the posteroventral cochlear nucleus: a kainic

548   acid lesion study in guinea pigs. *Journal of Comparative Neurology*, 487(4), 345-360.

549   Dimitrijevic, A. & Ross, B. (2008). Neural Generators of the Auditory Steady-State. *The*

550   *Auditory Steady-State Response: Generation, Recording, and Clinical Application*, *83*.

551   Ferragamo, M. J., Golding, N. L., & Oertel, D. (1998). Synaptic inputs to stellate cells in the

552   ventral cochlear nucleus. *Journal of neurophysiology*, 79(1), 51-63.

553   Fujino, K., & Oertel, D. (2001). Cholinergic modulation of stellate cells in the mammalian

554   ventral cochlear nucleus. *Journal of Neuroscience*, 21(18), 7372-7383.

555   Galambos, R. (1956). Suppression of auditory nerve activity by stimulation of efferent fibers to

556   cochlea. *Journal of Neurophysiology*, *19*(5), 424–437.

557   https://doi.org/10.1152/JN.1956.19.5.424

558   Guinan Jr, J. J. (2006). Olivocochlear efferents: anatomy, physiology, function, and the

559   measurement of efferent effects in humans. Ear and hearing, 27(6), 589-607.

560   Herdman, A. T., Lins, O., Van Roon, P., Stapells, D. R., Scherg, M., & Picton, T. W. (2002).

561   Intracerebral sources of human auditory steady-state responses. *Brain topography*, *15*(2),

562   69-86.

563   Kawase, T., Maki, A., Kanno, A., Nakasato, N., Sato, M., & Kobayashi, T. (2012). Contralateral

564   white noise attenuates 40-Hz auditory steady-state fields but not N100m in auditory evoked

565   fields. *NeuroImage*, *59*(2), 1037–1042.

566   https://doi.org/10.1016/J.NEUROIMAGE.2011.08.108

567   Kuwada, S., Anderson, J. S., Batra, R., Fitzpatrick, D. C., Teissier, N., & D'Angelo, W. R.

568   (2002). Sources of the scalp-recorded amplitude-modulation following response. *Journal of*

569   *the American Academy of Audiology*, *13*(04), 188-204.

570   Liberman, M.C. (1991). Central projections of auditory-nerve fibers of differing spontaneous

571   rate. I. An- teroventral cochlear nucleus. *The Journal of Comparative Neurology*,

572   313(2):240–258.

573   Liberman, MC and Kiang, NY. (1984). Single-neuron labeling and chronic cochlear pathology.

574   IV. Stereocilia damage and alterations in rate- and phase-level functions. *Hearing Research*,

575   16(1):75–90.

576   Maki, A., Kawase, T., & Kobayashi, T. (2009). Effects of contralateral noise on 40-Hz and 80-

577   Hz auditory steady-state responses. *Ear and Hearing*, *30*(5), 584–589.

578   https://doi.org/10.1097/AUD.0B013E3181ACFB57

579   May, B. J., Prell, G. S. L., & Sachs, M. B. (1998). Vowel representations in the ventral cochlear

580   nucleus of the cat: effects of level, background noise, and behavioral state. *Journal of*

581   *neurophysiology*, 79(4), 1755-1767.

582   Mulders, W. H., Harvey, A. R., & Robertson, D. (2007). Electrically evoked responses in onset

583   chopper neurons in guinea pig cochlear nucleus. *Journal of neurophysiology*, 97(5), 3288-

584   3297.

585   Oertel, D., Wright, S., Cao, X. J., Ferragamo, M., & Bal, R. (2011). The multiple functions of T

586   stellate/multipolar/chopper cells in the ventral cochlear nucleus. *Hearing research*, 276(1-

587   2), 61-69

588   Okoyama, Shigeo, Masao Ohbayashi, Makoto Ito, and Shinichi Harada. "Neuronal organization

589   of the rat inferior colliculus participating in four major auditory pathways." *Hearing*

590   *research* 218, no. 1-2 (2006): 72-80.

591   Parry, L. v., Maslin, M. R. D., Schaette, R., Moore, D. R., & Munro, K. J. (2019). Increased

592   auditory cortex neural response amplitude in adults with chronic unilateral conductive

593   hearing impairment. *Hearing Research*, *372*, 10–16.

594   https://doi.org/10.1016/J.HEARES.2018.01.016

595   Picton, T. W., John, M. S., Purcell, D. W., & Plourde, G. (2003). Human auditory steady-state

596   responses: the effects of recording technique and state of arousal. Anesthesia & Analgesia,

597   97(5), 1396-1402.

598   Rajan, R. (1988). Effect of Electrical Stimulation of the Crossed Olivocochlear Bundle on

599   Temporary Threshold Shifts in Auditory Sensitivity. I. Dependence on Electrical

600   Stimulation Parameters. In *JOURNALOF NEUROPHYSIOLOGY* (Vol. 60, Issue 2).

601   Robertson, D., & Mulders, W. H. (2011). Central effects of efferent activation. In *Auditory and*

602   *Vestibular Efferents* (pp. 291-312). Eds. D. K. Ryugo, R. R. Fay, and A. N. Popper.

603   Springer, New York, NY.

604   Ross, B., Herdman, A. T., & Pantev, C. (2005). Stimulus induced desynchronization of human

605   auditory 40-Hz steady-state responses. *Journal of Neurophysiology*, *94*(6), 4082–4093.

606   https://doi.org/10.1152/JN.00469.2005/ASSET/IMAGES/LARGE/Z9K0120551020007.JP

607   EG

608   Ross, B., Miyazaki, T., & Fujioka, T. (2012). Interference in dichotic listening: the effect of

609   contralateral noise on oscillatory brain networks. *European Journal of Neuroscience*, *35*(1),

610   106–118. https://doi.org/10.1111/J.1460-9568.2011.07935.X

611   Schofield, B. R. (2011). Central descending auditory pathways. In *Auditory and vestibular*

612   *efferents* (pp. 261-290). Eds. D. K. Ryugo, R. R. Fay, and A. N. Popper. Springer, New

613   York, NY.

614   Sheppard, A., Liu, X., Ding, D., & Salvi, R. (2018). Auditory central gain compensates for

615   changes in cochlear output after prolonged low-level noise exposure. Neuroscience letters,

616   687, 183-188.

617   Trussell, L. O. (2002). Cellular mechanisms for information coding in auditory brainstem nuclei.

618   In *Integrative functions in the mammalian auditory pathway* (pp. 72-98). Eds. Oertel, D., R.

619   R. Fay, and A. N. Popper. Springer, New York, NY.

620   Usubuchi, H., Kawase, T., Kanno, A., Yahata, I., Miyazaki, H., Nakasato, N., Kawashima, R., &

621   Katori, Y. (2014). Effects of Contralateral Noise on the 20-Hz Auditory Steady State

622   Response - Magnetoencephalography Study. *PLOS ONE*, *9*(6), e99457.

623   https://doi.org/10.1371/JOURNAL.PONE.0099457

624   Warren, E. H., & Liberman, M. C. (1989). Effects of contralateral sound on auditory-nerve

625   responses. I. Contributions of cochlear efferents. *Hearing Research*, *37*(2), 89–104.

626   https://doi.org/10.1016/0378-5955(89)90032-4

627   Winslow, R. L., & Sachs, M. B. (1987). Effect of electrical stimulation of the crossed

628   olivocochlear bundle on auditory nerve response to tones in noise. *Journal of*

629   *neurophysiology*, *57*(4), 1002-1021

630

Figure Captions

632   **Figure 1: Schematic of the experimental protocol**. Both 40 and 80 Hz clicks were

633   presented in short (1.5 s) and long durations (4 mins) at 65 dB ppSPL, with and without a 60 dB

634   SPL broadband noise in the contralateral ear. Clicks were presented in positive and negative

635   polarities to facilitate ASSR averaging. Each stimulus duration was separated by 0.5 s of silence.

636

637   **Figure 2: Stimulus vs. OAE change**. Stimulus amplitude change as a function of OAE

638   amplitude change for (A) 40 Hz click-rate, long stimulus duration (B) 40 Hz click-rate, short

639   stimulus duration (C) 80 Hz click-rate, long stimulus duration (D) 80 Hz click-rate, short

640   stimulus duration. Open circles represent individual participants. A black solid regression line

641   represents a significant relationship between variables. A black dashed regression line represents

642   a nonsignificant relationship between variables. The resulting correlation coefficient (r) and p-

643   value are presented in each panel. In panel C, the blue solid regression line correlation when the

644   outlier is included.

645   **Figure 3: Response amplitude change with contralateral noise.** ASSR in the top four

646   panels and OAEs in the bottom four panels. Columns separate long and short duration conditions

647   and rows separate 40 and 80 Hz click-rates. Black circles (40 Hz click-rate) and black triangles

648   (80 Hz click-rate) indicate group means and grey lines represent individual participants. Error
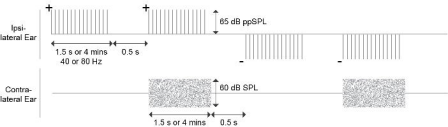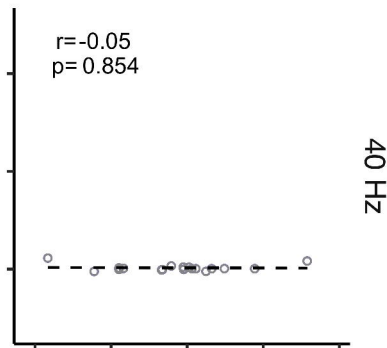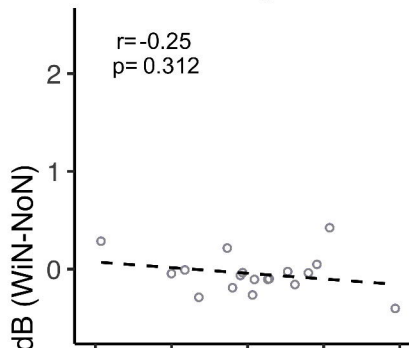
649   bars represent ± one standard deviation. Asterisks denote a significant difference in amplitude

650   between with- (WiN) and no-noise (NoN) conditions.

651   **Figure 4: ASSRs vs. OAE amplitude change**. (A) 40 Hz click-rate, long stimulus duration

652   (B) 40 Hz click-rate, short stimulus duration (C) 80 Hz click-rate, long stimulus duration (D) 80

653   Hz click-rate, short stimulus duration. Open circles represent individual participants. A black

654   solid fit line represents a significant relationship between variables. A black dashed fit line

655   represents a nonsignificant relationship between variables.

656   **Figure 5: Long vs. short duration.** Amplitude changes in the long stimulus durations as

657   a function of amplitude change in the short stimulus durations are plotted for (A) 40 Hz click-

658   rate, ASSRs (B) 40 Hz click-rate, OAEs (C) 80 Hz click-rate, ASSRs (D) 80 Hz click-rate,

659   OAEs. Open circles represent individual participants. A black solid regression line indicates a

660   significant relationship between the two variables. A black dashed regression line indicates a

661   non-significant relationship between the two variables.

662   **Figure 6: 40 Hz vs. 80 Hz.** Amplitude changes at 80 Hz click-rate as a function of

663   amplitude change at 40 Hz click-rate for (A) ASSRs, long stimulus duration (B) ASSRs, short

664   stimulus duration (C) OAEs, long stimulus duration (D) ASSRs, short stimulus duration. Open

665   circles represent individual participants. A black solid regression line indicates a significant

666   relationship between the two variables. A black dashed regression line indicates a non-significant

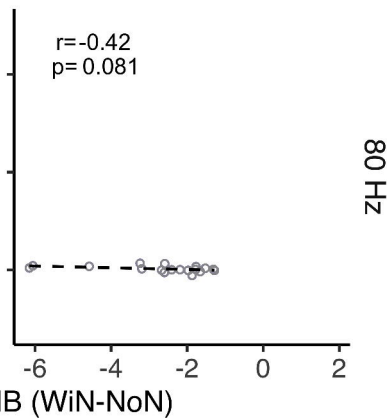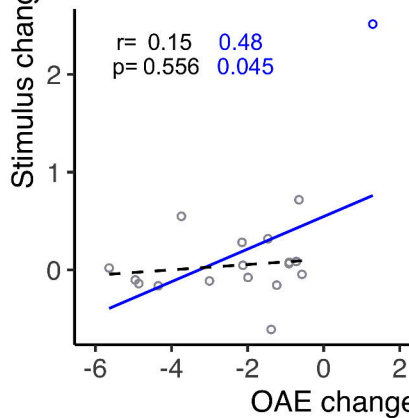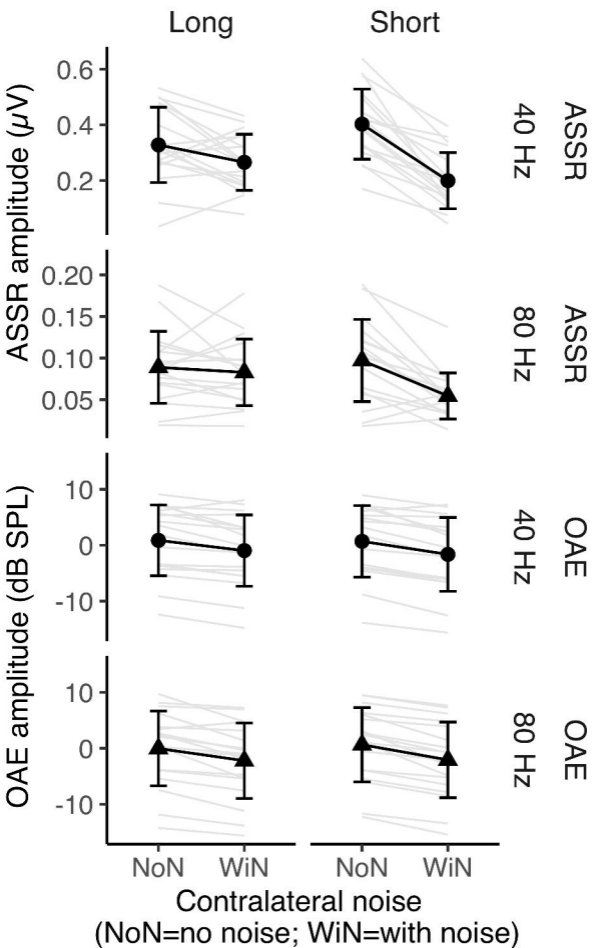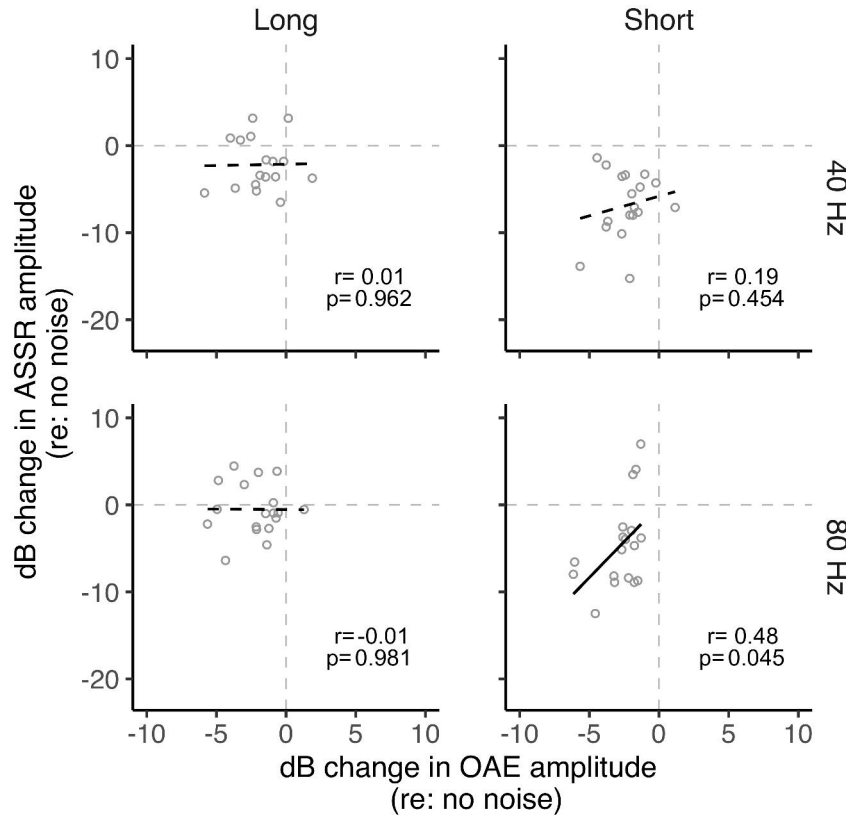667   relationship between the two variables.

Ipsi-
lateral Ear

+   +   65 dB ppSPL

1.5 s or 4 mins   0.5 s
40 or 80 Hz

−   −

Contra-
lateral Ear

60 dB SPL

1.5 s or 4 mins   0.5 s